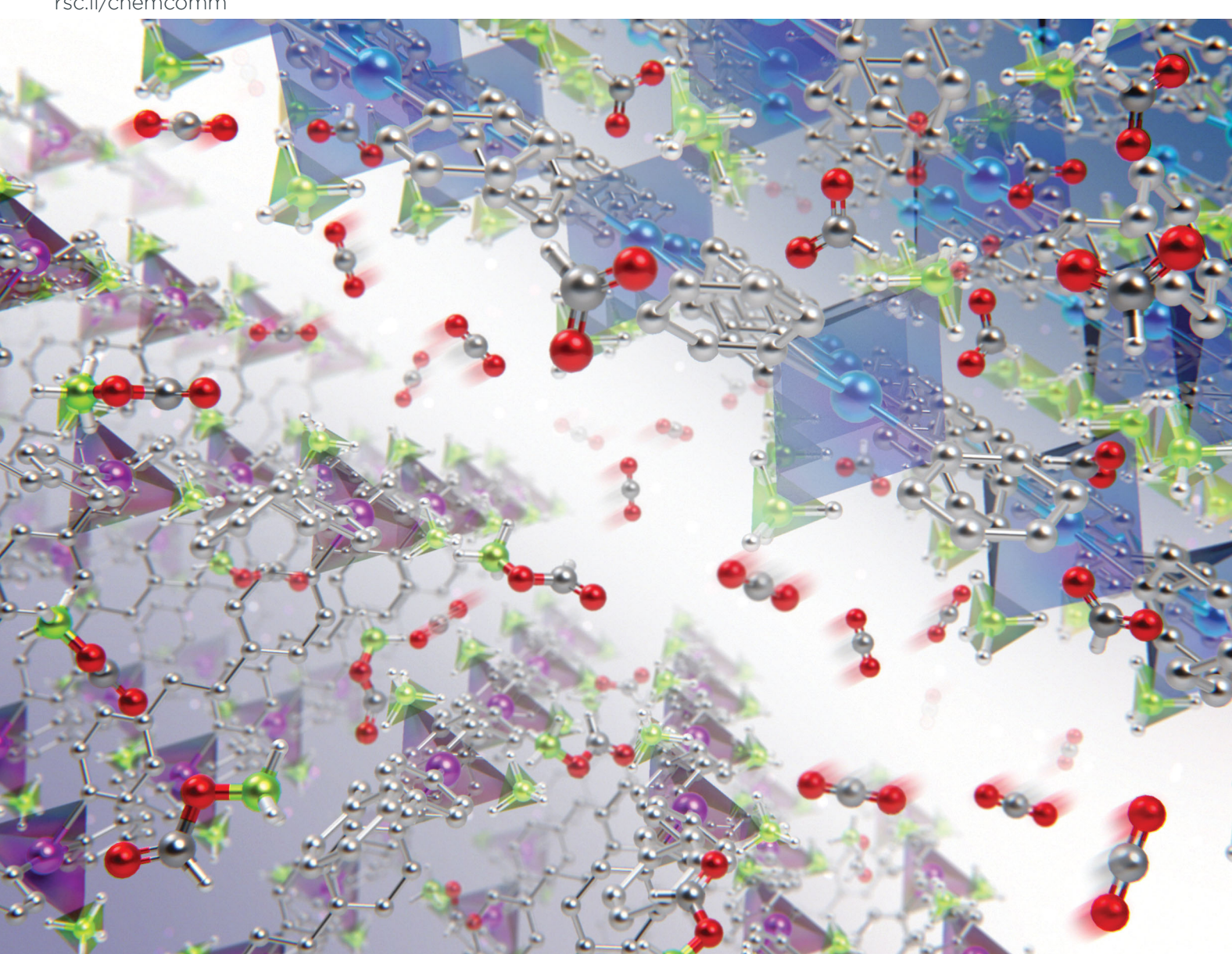
Volume 56 Number 38 11 May 2020 Pages 5069-5196

# ChemComm

Chemical Communications

rsc.li/chemcomm



ISSN 1359-7345



#### COMMUNICATION

Satoshi Horike et al. Reactivity of borohydride incorporated in coordination polymers toward carbon dioxide

# ChemComm



## COMMUNICATION

View Article Online



**Cite this:** *Chem. Commun.*, 2020, **56**, 5111

Received 6th March 2020, Accepted 6th April 2020

DOI: 10.1039/d0cc01753a

rsc.li/chemcomm

# Reactivity of borohydride incorporated in coordination polymers toward carbon dioxide†

Kentaro Kadota. Da Easan Siyaniah Dab and Satoshi Horike \*\*D\*\* \*\*D\*\*Cde

Borohydride (BH $_4$ <sup>-</sup>)-containing coordination polymers converted CO $_2$  into HCO $_2$ <sup>-</sup> or [BH $_3$ (OCHO)] $^-$ , whose reaction routes were affected by the electronegativity of metal ions and the coordination mode of BH $_4$  $^-$ . The reactions were investigated using thermal gravimetric analysis under CO $_2$  gas flow, infrared spectroscopy, and NMR experiments.

Conversion of carbon dioxide ( $CO_2$ ) into valuable chemicals is a key to realize a sustainable society. <sup>1,2</sup> In particular, it is essential to establish chemical reactions that transform  $CO_2$  into various types of chemical moieties under mild conditions. <sup>3</sup> However, the inherent inertness of  $CO_2$  has hampered the utilization of  $CO_2$  in transformation reactions. To overcome the inertness, various catalytic and stoichiometric reactions have been widely studied in both solution and the solid-state, including metals, metal oxides, <sup>4</sup> metal complexes, <sup>5,6</sup> and metal-free organic molecules. <sup>7</sup>

Borohydride (BH<sub>4</sub><sup>-</sup>), a hydride-based complex anion, has been commonly utilized as a reducing agent. In the solution phase, metal borohydrides (MBHs) stoichiometrically react with CO<sub>2</sub> at ambient temperatures and pressures. BH<sub>4</sub> in solution is able to convert CO<sub>2</sub> into chemical species such as formate (HCO<sub>2</sub><sup>-</sup>) and formylhydroborate ([BH<sub>4-x</sub>(OCHO)<sub>x</sub>]<sup>-</sup>, x = 1, 2 and 3) depending on the reaction conditions, *e.g.* counter cations, temperatures,

solvents, and pressures. \$^{8,9,12}\$ The solid-state reactivity of BH<sub>4</sub> toward CO<sub>2</sub> is also interesting from the viewpoint of heterogeneous catalysts and CO<sub>2</sub> scrubbers. Nevertheless, limited studies have been performed on the solid-state reactivity of MBHs toward CO<sub>2</sub>.  $^{13,14}$  This is because slow diffusion of CO<sub>2</sub> in dense MBHs results in low reactivity under mild conditions.  $^{14}$  Although porous structures are advantageous for the diffusion of CO<sub>2</sub>, MBHs with the porous structure are limited except for a few examples,  $e.g. \ \gamma$ -Mg(BH<sub>4</sub>)<sub>2</sub>.  $^{14,15}$ 

Coordination polymers (CPs) and metal-organic frameworks (MOFs) are crystalline solids constructed from metal ions and bridging organic linkers. <sup>16–18</sup> Their open structures have offered an attractive platform for various gas-solid reactions, such as CO<sub>2</sub> sorption <sup>19–21</sup> and post-synthetic modification. <sup>22,23</sup> In addition, rich structural and chemical tunability of CPs demonstrated the controlled reactivity of reactive species, *e.g.* radicals, <sup>24,25</sup> imines, <sup>26</sup> and photoactive metal complexes. <sup>27</sup> CPs are a promising platform for solid-gas reactions between BH<sub>4</sub><sup>-</sup> and CO<sub>2</sub>. BH<sub>4</sub><sup>-</sup>-containing CPs are constructed from metal ions (*e.g.* Mg<sup>2+</sup>, Ca<sup>2+</sup>, Mn<sup>2+</sup>, Zn<sup>2+</sup>, and Th<sup>4+</sup>) and N-based neutral linkers show various types of the chemical environment of BH<sub>4</sub><sup>-</sup>.<sup>28–30</sup> Here, we investigate the reactivity of BH<sub>4</sub><sup>-</sup>-containing CPs to convert CO<sub>2</sub> into HCO<sub>2</sub><sup>-</sup> or [BH<sub>3</sub>(OCHO)]<sup>-</sup> under mild conditions depending on their structures

 $[M(BH_4)_2(pyz)_2]$  (**M-pyz**,  $M = Mg^{2+}$ ,  $Ca^{2+}$ , pyz = pyrazine)<sup>28,29</sup> were selected to investigate the influence of metal ions on the reactivity of  $BH_4^-$  toward  $CO_2$ . The metal ion center shows an octahedral geometry and the two  $BH_4^-$  ions coordinate in the axial positions (Fig. 1A). The extended structure of **M-pyz** comprises a 2D square grid constructed by  $[M_4pyz_4]$  units (Fig. 1B). The electronic properties and reactivity of  $BH_4^-$  are influenced by the electronegativity of counter metal ions.<sup>31,32</sup> Attempts at the synthesis of isostructural **M-pyz** were made using a  $Mn^{2+}$ -based MBH precursor.  $[Mn(BH_4)_2\cdot 3THF]\cdot NaBH_4$  was prepared following the literature methods.<sup>33</sup> The general synthetic method involves mechanochemical milling of the MBH precursor and pyz under Ar. **Mg-pyz** was previously

<sup>&</sup>lt;sup>a</sup> Department of Molecular Engineering, Graduate School of Engineering, Kyoto University, Katsura, Nishikyo-ku, Kyoto 615-8510, Japan

b Institute for Integrated Cell-Material Sciences, Institute for Advanced Study, Kyoto University, Yoshida, Sakyo-ku, Kyoto 606-8501, Japan. E-mail: horike@icems.kyoto-u.ac.jp

<sup>&</sup>lt;sup>c</sup> AIST-Kyoto University Chemical Energy Materials Open Innovation Laboratory (ChEM-OIL), National Institute of Advanced Industrial Science and Technology (AIST), Yoshida-Honmachi, Sakyo-ku, Kyoto 606-8501, Japan

<sup>&</sup>lt;sup>d</sup> Department of Synthetic Chemistry and Biological Chemistry, Graduate School of Engineering, Kyoto University, Katsura, Nishikyo-ku, Kyoto 615-8510, Japan

<sup>&</sup>lt;sup>e</sup> Department of Materials Science and Engineering, School of Molecular Science and Engineering, Vidyasirimedhi Institute of Science and Technology, Rayong 21210, Thailand

<sup>†</sup> Electronic supplementary information (ESI) available. See DOI: 10.1039/d0cc01753a

Communication ChemComm

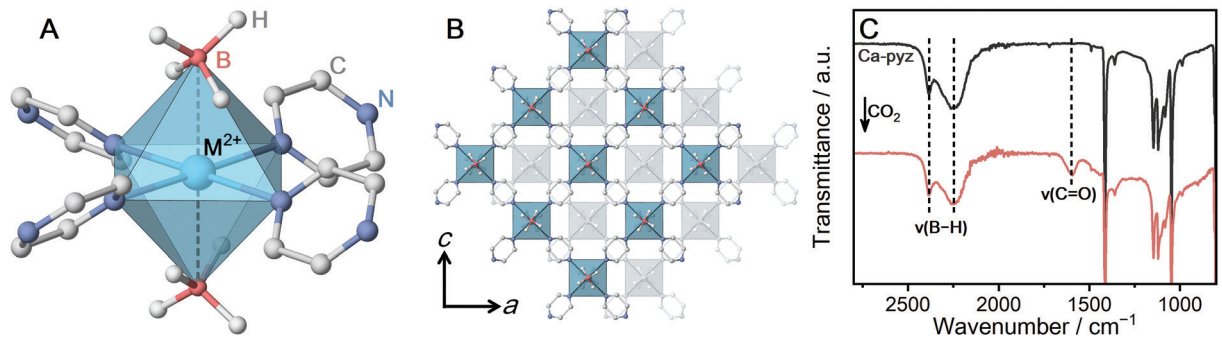


Fig. 1 (A) Local coordination geometry of **M-pyz** (M =  $Mg^{2+}$ ,  $Ca^{2+}$ ,  $Mn^{2+}$ ). (B) ABAB stacking structure of the extended 2D layers of **M-pyz** (M =  $Mg^{2+}$ ,  $Ca^{2+}$ ,  $Mn^{2+}$ ). (C) IR spectra of **Ca-pyz** before and after CO<sub>2</sub> adsorption at 25 °C.

synthesized in the solution phase, whereas the solvent-free conditions afford a highly crystalline product as well (Fig. S1, ESI†). The powder X-ray diffraction (PXRD) pattern of **Mn-pyz** shows a good agreement with that of **Mg-pyz** (Fig. S1, ESI†).

The solid-state synthesis of M-pyz proceeds without solvents at 25 °C within 30 min. The fast reaction kinetics in the solidstate is ascribed to the low melting point of pyz (52 °C). The lower melting point of reactants leads to higher molecular mobility, enhancing the reactivity in the solid-state.<sup>34</sup> Mechanical milling is useful to synthesize CPs from MBHs because most of the MBHs are poorly soluble in common organic solvents. The thermal properties were characterized by thermal gravimetric analysis (TGA) under N2 (Fig. S2, ESI†). Each compound exhibits a weight loss at relatively low temperatures; 50, 70, and 70 °C for Mg-, Mn-, and Ca-pyz due to the low boiling point of pyz (115  $^{\circ}$ C). Isothermal TGA measurements at 40 °C under N<sub>2</sub> indicate that Ca-pyz shows higher thermal stability than Mn-pyz (weight loss after 6 hours; 0.2 vs. 3.2 wt%, Fig. S3, ESI†). In the case of MBHs, electropositive metal ions construct MBHs with higher thermal stability.35 Meanwhile, in the case of BH<sub>4</sub>--containing CPs, the strength of the coordination bonds is also essential. The Hard and Soft Acids and Bases (HSAB) theory reveals that electropositive metal ions (hard acids) form weaker coordination bonds with nitrogen-based linkers (soft bases) such as pyz. Therefore, the trend of thermal stability for M-pyz does not simply follow the electronegativity of metal ions (thermal stability: Mg < Mn < Ca, Pauling electronegativity: Ca < Mg < Mn).

To characterize the chemical environment of  $BH_4^-$  in the CP, solid-state  $^{11}B$  magic angle spinning (MAS) nuclear magnetic resonance (NMR) was carried out on non-paramagnetic Ca-pyz. The  $^{11}B$  NMR spectrum of Ca-pyz displays a peak at -36 ppm corresponding to the signal of  $BH_4^-$  (Fig. S4, ESI†). The total charge on  $BH_4^-$  is correlated with the chemical shift of  $^{11}B$  NMR: electron-rich  $BH_4^-$  shows a peak in a lower frequency.  $^{31}$  The low-frequency shift of the  $^{11}B$  peak indicates that  $BH_4^-$  in Ca-pyz is more electron-rich than  $Ca(BH_4)_2$ . In the framework of Ca-pyz, the Lewis acidity of  $Ca^{2+}$  was reduced by electron donation from the coordinating pyz molecules, which leads to the formation of electron-rich  $BH_4^-$ .  $^{29}$ 

 ${
m CO_2}$  adsorption measurement was carried out to evaluate the reactivity of Ca-pyz in gas-solid equilibrium. The  ${
m CO_2}$ 

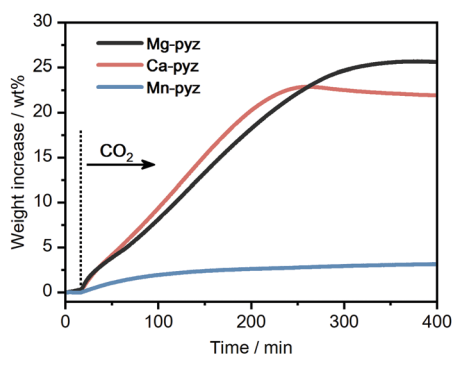


Fig. 2 Isothermal TGA profiles of **M-pyz** ( $M = Mg^{2+}$ ,  $Ca^{2+}$ ,  $Mn^{2+}$ ) under  $CO_2$  flow (0.1 MPa, 30 mL min<sup>-1</sup>) at 40 °C.

isotherm at 25 °C displays irreversible adsorption (7 mL g<sup>-1</sup> at 100 kPa), which is characteristic of chemisorption behavior (Fig. S5, ESI†). The IR spectrum of Ca-pyz after CO<sub>2</sub> adsorption displays a new peak at 1600 cm<sup>-1</sup>, corresponding to C=O stretching (Fig. 1C). The solid-state  $^{1}\text{H}^{-13}\text{C}$  cross-polarization (CP) MAS NMR spectrum of Ca-pyz after CO<sub>2</sub> adsorption shows peaks at 170 and 145 ppm. The peaks correspond to the signals of HCO<sub>2</sub><sup>-</sup> and pyz, respectively (Fig. S6, ESI†). The results indicate that BH<sub>4</sub><sup>-</sup> in Ca-pyz reduces CO<sub>2</sub> to HCO<sub>2</sub><sup>-</sup> with the release of diborane (B<sub>2</sub>H<sub>6</sub>) as a by-product. O

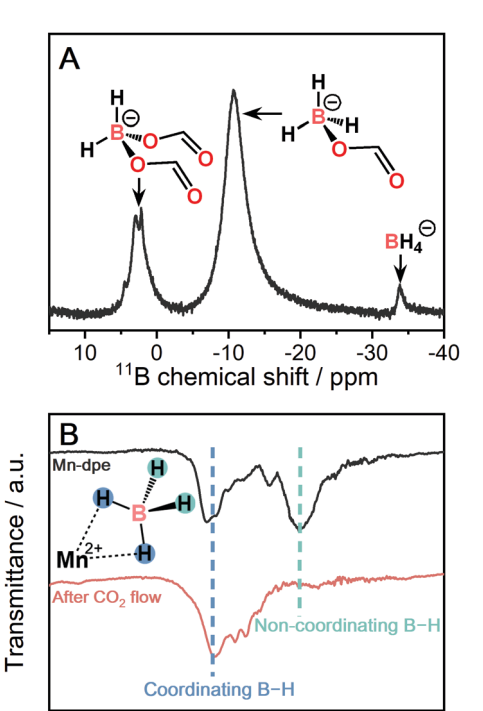
The kinetic reactivity of M-pvz toward CO2 was evaluated using isothermal TGA under CO2 flow. Fig. 2 displays the TGA profiles of each powder sample (10 mg) under CO<sub>2</sub> flow (0.1 MPa, 30 mL min<sup>-1</sup>) at 40 °C. Mg-pyz and Ca-pyz exhibit higher weight increases than Mn-pyz (25.5, 21.9, and 3.2 wt% after 400 min, respectively). Ca-pyz was amorphous after the CO2 reaction, as confirmed by PXRD (Fig. S7, ESI†). To identify the chemical species after the CO<sub>2</sub> reaction, solution NMR was carried out on Ca-pyz dissolved in DMSO- $d_6$ . The solution  $^{13}$ C NMR spectrum of Ca-pyz after the CO<sub>2</sub> reaction displays peaks at 167, 146, 53, 50, 47 and 44 ppm (Fig. S8, ESI†). The peaks at 167 and 146 ppm correspond to the <sup>13</sup>C signals of HCO<sub>2</sub><sup>-</sup> and pyz, respectively. The peak at 47 ppm is assigned to piperazine formed by the reduction of pyz by B<sub>2</sub>H<sub>6</sub>, whereas the rest of the peaks are not able to be assigned.<sup>29,37</sup> The higher reactivity of Ca-pyz toward CO2 is attributed to the preferable electronic ChemComm Communication

interaction between Ca<sup>2+</sup> (hard acid) and HCO<sub>2</sub><sup>-</sup> (hard base) rather than BH<sub>4</sub> (soft base).

The formation of  $[BH_{4-x}(OCHO)_x]^-$  from  $BH_4^-$  and  $CO_2$  was investigated at a  $BH_4$ --containing CP. Given that  $[BH_{4-x}(OCHO)_x]$ is bulky than  $HCO_2^-$ ,  $[Mn(BH_4)_2(dpe)_{1.5}]$  (Mn-dpe, dpe = dipyridylethane) having voids was selected.  $^{28}$  The two  $\mathrm{BH_4}^-$  ions coordinate to the Mn<sup>2+</sup> center in a bidentate manner, which was confirmed by single-crystal X-ray diffraction (SC-XRD) in Fig. 3A. The extended structure of Mn-dpe comprises a 1D ladder constructed from [Mn4dpe4] units (Fig. 3B). The coordination mode of  $BH_4^-$  was confirmed by IR spectroscopy as well. The IR spectrum of Mn-dpe displays two stretching peaks in the B-H stretching region at 2378 and 2127 cm<sup>-1</sup>, respectively (Fig. 4B). The peak at 2378 cm<sup>-1</sup> corresponds to the B-H bond coordinating to the Mn<sup>2+</sup> center, whereas the peak at 2127 cm<sup>-1</sup> corresponds to the noncoordinating B-H.38 In contrast to the broadened B-H stretching peak of Ca-pyz (Fig. 1C), Mn-dpe displays distinct two peaks of B-H stretching, which is originated from a stronger binding interaction between Mn<sup>2+</sup> (soft acid) and BH<sub>4</sub><sup>-</sup> (soft base).

The kinetic curve of the CO2 reaction with Mn-dpe was collected using the same procedure as M-pvz (Fig. 3B). Mn-dpe demonstrates a weight increase of 26.2 wt% after 600 min at 40 °C, which corresponds to a value of the 1.1:1 molar ratio of reacted CO<sub>2</sub> per BH<sub>4</sub><sup>-</sup>. After the CO<sub>2</sub> reaction, Mn-dpe shows small diffraction peaks different from the original peaks (Fig. S9, ESi†). Solution <sup>11</sup>B NMR measurement was carried out to determine the chemical species after the CO2 reaction. The <sup>11</sup>B{<sup>1</sup>H} NMR spectrum of digested **Mn-dpe** after the CO<sub>2</sub> reaction displays the peaks at -33, -11, and 2.2 ppm in Fig. 4A. The broad peaks were observed due to the paramagnetic effect of Mn<sup>2+</sup>. The <sup>11</sup>B peaks correspond to BH<sub>4</sub>-, [BH<sub>3</sub>(OCHO)]<sup>-</sup> and [BH<sub>2</sub>(OCHO)<sub>2</sub>]<sup>-</sup>, respectively. 9,39 Successive CO<sub>2</sub> insertions into the B-H bond of BH<sub>4</sub><sup>-</sup> produce  $[BH_{4-x}(OCHO)_x]^-$ , and the number of reacted  $CO_2$  molecules is affected by the reaction conditions such as pressure and temperature in the solution phase.<sup>8,9</sup> The reaction of NaBH<sub>4</sub> in acetonitrile with 0.1 MPa of CO<sub>2</sub> for 10 minutes produces [BH(OCHO)<sub>3</sub>] as a major product, and [BH<sub>3</sub>(OCHO)] is not observed. This is because all the hydrogen atoms of BH<sub>4</sub> dissociated in acetonitrile are available for the reaction with CO<sub>2</sub>. On the other hand, in the case of Mn-dpe, two of the hydrogen atoms of BH<sub>4</sub> are pinned with the Mn<sup>2+</sup> center by

This journal is @ The Royal Society of Chemistry 2020



Wavenumber / cm<sup>-</sup> Fig. 4 (A) Solution <sup>11</sup>B{<sup>1</sup>H} NMR of digested **Mn-dpe** after CO<sub>2</sub> reaction. (B) IR spectra of Mn-dpe before and after the CO<sub>2</sub> reaction.

2200

2000

1800

2400

2800

2600

a coordination bond as confirmed by SC-XRD and IR spectroscopy. After the CO<sub>2</sub> reaction, a non-coordinating B-H stretching peak was not observed, and this is because of the reaction with CO<sub>2</sub> to form [BH<sub>3</sub>(OCHO)]<sup>-</sup> and [BH<sub>2</sub>(OCHO)<sub>2</sub>]<sup>-</sup> in Fig. 4B. The coordinating B-H stretching peak is preserved after the CO2 reaction, indicating the coordinating bonds between Mn<sup>2+</sup> and [BH<sub>3</sub>(OCHO)]<sup>-</sup> or [BH<sub>2</sub>(OCHO)<sub>2</sub>]<sup>-</sup>. A sluggish kinetics of dense NaBH<sub>4</sub> in the solid-state toward CO2 indicates that the open structure of Mn-dpe is essential for the diffusion of CO<sub>2</sub> (Fig. 3C). Based on the results, the reaction between Mn-dpe and CO2 to produce [BH<sub>3</sub>(OCHO)]<sup>-</sup> and [BH<sub>2</sub>(OCHO)<sub>2</sub>]<sup>-</sup> is proposed (Fig. S11, ESI†). The results indicate that the anisotropic coordination geometry of BH<sub>4</sub> in Mn-dpe affects the reaction route with CO2.

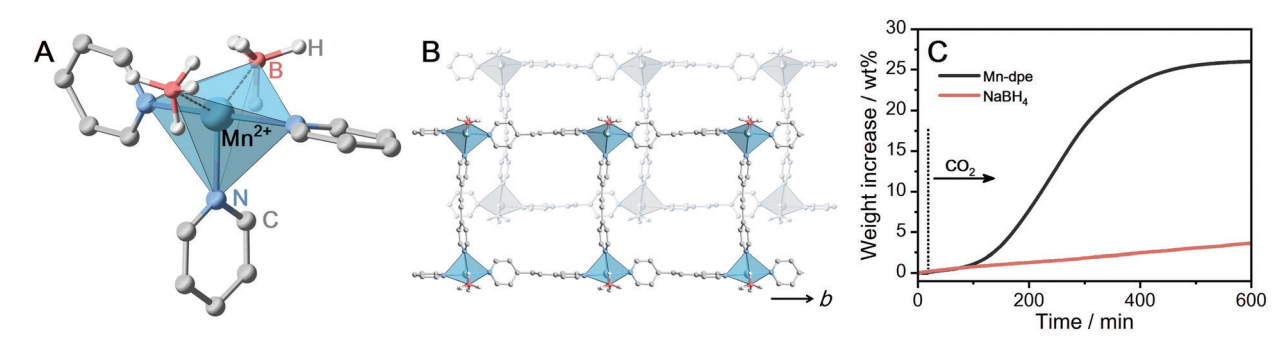


Fig. 3 (A) Local coordination geometry of Mn-dpe. (B) Packing structure of the extended 1D ladders of Mn-dpe. (C) Isothermal TGA profiles of Mn-dpe and NaBH<sub>4</sub> under CO<sub>2</sub> flow (0.1 MPa, 30 mL min<sup>-1</sup>) at 40 °C.

Communication ChemComm

In conclusion, we demonstrated the reactivity of BH<sub>4</sub> toward CO2 which is correlated with the crystal structures of BH<sub>4</sub>--containing coordination polymers. The reactivity of  $[M(BH_4)_2(pyrazine)_2]$   $(M = Mg^{2+}, Mn^{2+}, Ca^{2+})$  and [Mn(BH<sub>4</sub>)<sub>2</sub>(dipyridylethane)<sub>1.5</sub>] toward CO<sub>2</sub> at 40 °C was investigated by using isothermal TGA under CO2 flow, IR and NMR. BH<sub>4</sub> in [Ca(BH<sub>4</sub>)<sub>2</sub>(pyrazine)<sub>2</sub>] converted CO<sub>2</sub> into HCO<sub>2</sub><sup>-</sup>. The BH<sub>4</sub><sup>-</sup> pinned by coordination bonds with Mn<sup>2+</sup> in  $[Mn(BH_4)_2(dipyridylethane)_{1,5}]$  regulated the successive CO<sub>2</sub> insertion reaction and produced [BH<sub>3</sub>(OCHO)]<sup>-</sup> as a major species. The structural diversity of coordination polymers provides a new approach to regulate the reaction routes between BH<sub>4</sub><sup>-</sup> and CO<sub>2</sub> in the solid-state.

The work was supported by the Japan Society of the Promotion of Science (ISPS) for a Grant-in-Aid for Scientific Research (B) (JP18H02032), the Challenging Research (Exploratory) (JP19K22200) from the Ministry of Education, Culture, Sports, Science and Technology, Japan, and Strategic International Collaborative Research Program (SICORP), the Adaptable and Seamless Technology Transfer Program through Target-driven R&D (A-STEP) from the Japan Science and Technology, Japan, Inamori Research Grants, and Tokuyama Science Foundation.

#### Conflicts of interest

The authors declare no conflict of interest.

### References

- 1 T. Sakakura, J.-C. Choi and H. Yasuda, Chem. Rev., 2007, 107, 2365-2387.
- 2 J. Artz, T. E. Muller, K. Thenert, J. Kleinekorte, R. Meys, A. Sternberg, A. Bardow and W. Leitner, Chem. Rev., 2018, 118, 434-504.
- 3 Q. Liu, L. Wu, R. Jackstell and M. Beller, Nat. Commun., 2015, 6, 5933.
- 4 J. L. White, M. F. Baruch, J. E. P. Iii, Y. Hu, I. C. Fortmeyer, J. E. Park, T. Zhang, K. Liao, J. Gu, Y. Yan, T. W. Shaw, E. Abelev and A. B. Bocarsly, Chem. Rev., 2015, 115, 12888-12935.
- 5 A. J. Morris, G. J. Meyer and E. Fujita, Acc. Chem. Res., 2009, 42, 1983-1994.
- 6 B. J. Cook, G. N. Di Francesco, K. A. Abboud and L. J. Murray, J. Am. Chem. Soc., 2018, 140, 5696-5700.
- 7 D. W. Stephan and G. Erker, Angew. Chem., Int. Ed., 2015, 54, 6400-6441.
- 8 G. La Monica, G. A. Ardizzoia, F. Cariati, S. Cenini and M. Pizzotti, Inorg. Chem., 1985, 24, 3920-3923.
- 9 I. Knopf and C. C. Cummins, Organometallics, 2015, 34, 1601-1603.
- 10 S. Murugesan, B. Stöger, M. Weil, L. F. Veiros and K. Kirchner, Organometallics, 2015, 34, 1364-1372.

- 11 J. G. Burr, W. G. Brown and H. E. Heller, J. Am. Chem. Soc., 1950, 72, 2560-2562.
- 12 K. Kadota, N. T. Duong, Y. Nishiyama, E. Sivaniah and S. Horike, Chem. Commun., 2019, 55, 9283-9286.
- 13 J. Zhang and J. W. Lee, Carbon, 2013, 53, 216-221.
- 14 J. G. Vitillo, E. Groppo, E. G. Bardaji, M. Baricco and S. Bordiga, Phys. Chem. Chem. Phys., 2014, 16, 22482-22486.
- 15 Y. Filinchuk, B. Richter, T. R. Jensen, V. Dmitriev, D. Chernyshov and H. Hagemann, Angew. Chem., Int. Ed., 2011, 50, 11162-11166.
- 16 S. Kitagawa, R. Kitaura and S. Noro, Angew. Chem., Int. Ed., 2004, 43, 2334-2375.
- 17 O. M. Yaghi, M. O'Keeffe, N. W. Ockwig, H. K. Chae, M. Eddaoudi and J. Kim, Nature, 2003, 423, 705-714.
- 18 G. Férey, Chem. Soc. Rev., 2008, 37, 191-214.
- 19 T. M. McDonald, J. A. Mason, X. Kong, E. D. Bloch, D. Gygi, A. Dani, V. Crocella, F. Giordanino, S. O. Odoh, W. S. Drisdell, B. Vlaisavljevich, A. L. Dzubak, R. Poloni, S. K. Schnell, N. Planas, K. Lee, T. Pascal, L. F. Wan, D. Prendergast, J. B. Neaton, B. Smit, J. B. Kortright, L. Gagliardi, S. Bordiga, J. A. Reimer and J. R. Long, Nature, 2015, 519, 303-308.
- 20 A. Phan, C. J. Doonan, F. J. Uribe-Romo, C. B. Knobler, M. O'Keeffe and O. M. Yaghi, Acc. Chem. Res., 2010, 43, 58-67.
- 21 E. González-Zamora and I. A. Ibarra, Mater. Chem. Front., 2017, 1, 1471-1484.
- 22 M. Servalli, M. Ranocchiari and J. A. Van Bokhoven, Chem. Commun., 2012, 48, 1904-1906.
- 23 V. Guillerm, H. Xu, J. Albalad, I. Imaz and D. Maspoch, J. Am. Chem. Soc., 2018, 140, 15022-15030.
- 24 H. Sato, R. Matsuda, K. Sugimoto, M. Takata and S. Kitagawa, Nat. Mater., 2010, 9, 661-666.
- 25 T. B. Faust and D. M. D'Alessandro, RSC Adv., 2014, 4, 17498-17512.
- 26 T. Haneda, M. Kawano, T. Kawamichi and M. Fujita, J. Am. Chem. Soc., 2008, 130, 1578-1579.
- 27 S. S. Kaye and J. R. Long, J. Am. Chem. Soc., 2008, 130, 806-807.
- 28 K. Kadota, N. T. Duong, Y. Nishiyama, E. Sivaniah, S. Kitagawa and S. Horike, Chem. Sci., 2019, 10, 6193-6198.
- 29 M. J. Ingleson, J. P. Barrio, J. Bacsa, A. Steiner, G. R. Darling, J. T. A. Jones, Y. Z. Khimyak and M. J. Rosseinsky, Angew. Chem., Int. Ed., 2009, 48, 2012-2016.
- 30 J. McKinven, G. S. Nichol and P. L. Arnold, Dalton Trans., 2014, 43, 17416-17421.
- 31 Z. Łodziana, P. Błoński, Y. Yan, D. Rentsch and A. Remhof, J. Phys. Chem. C, 2014, 118, 6594-6603.
- 32 Y. Nakamori, H. Li, K. Miwa, S.-I. Towata and S.-I. Orimo, Mater. Trans., 2006, 47, 1898-1901.
- 33 V. D. Makhaev, A. P. Borisov, T. P. Gnilomedova, É. B. Lobkovskii and A. N. Chekhlov, Bull. Acad. Sci. USSR, Div. Chem. Sci., 1987, 36, 1582-1586.
- 34 A. Pichon and S. L. James, CrystEngComm, 2008, 10, 1839-1847.
- 35 Y. Nakamori, K. Miwa, A. Ninomiya, H. Li, N. Ohba, S. Towata, A. Züttel and S. Orimo, Phys. Rev. B: Condens. Matter Mater. Phys., 2006, 74, 045126.
- 36 J. G. Bell, S. A. Morris, F. Aidoudi, L. J. McCormick, R. E. Morris and K. M. Thomas, J. Mater. Chem. A, 2017, 5, 23577-23591.
- 37 B. Chatterjee and C. Gunanathan, J. Chem. Sci., 2019, 131, 118.
- 38 T. J. Marks and J. R. Kolb, Chem. Rev., 1977, 77, 263-293.
- 39 C. V. Picasso, D. A. Safin, I. Dovgaliuk, F. Devred, D. Debecker, H.-W. Li, J. Proost and Y. Filinchuk, Int. J. Hydrogen Energy, 2016, 41, 14377-14386.